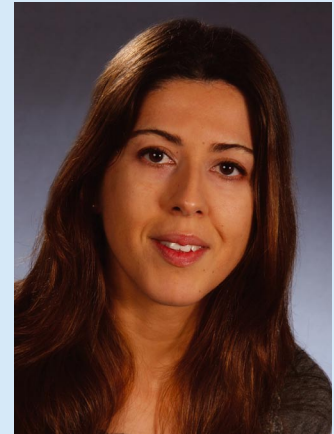


# Comparison Between LES Modelling and Experimental Observations under Offshore Conditions

B. Cañadillas, T. Neumann; DEWI GmbH, Wilhelmshaven



B. Cañadillas

ENGLISH

## Introduction

Over the next years, an increasing tendency towards offshore wind energy is expected world-wide [1]. One of the main reasons for 'going offshore' is the higher and more constant wind resource at sea than on land, resulting in significantly higher wind energy production per unit installed. At the same time, offshore wind farms are more costly to install and maintain compared to onshore wind farms. Both installation and maintenance depend significantly on the marine conditions, i.e. the marine atmospheric boundary layer which e.g. sets the limits for access and gives a basis for the layout of the wind turbine. Therefore, to make offshore wind farms economically feasible it is necessary to have a detailed knowledge of offshore conditions. Current knowledge of offshore conditions is very limited compared to conditions on land and this has placed growing importance on the necessity for research in this field.

In this work, Large-Eddy Simulations (LESs) have been performed and compared with observational data (FINO1 database), which will help us to gain a further understanding of offshore conditions. Shear-driven flows (under neutral and stable regimes) have been considered here because

of their importance in wind energy applications. Not only mean values (profiles) are compared in this study but also the turbulence unsteady effects are checked by using a statistical approach.

Overall, the model reproduces the most important flow characteristics under neutral and weak stable conditions at the model resolution used. The LES investigation will give us further insight into the physics of the marine atmospheric boundary layer and leads to a deeper understanding of measurement campaigns like FINO1. It shall help us in answering questions like "how representative is the data we receive at FINO1", "how will be the correlation of nearby measurements", "how can we model and predict wind farm turbulences" or "how will other measurement methods like LIDAR correlate with cup anemometry", which may lead the way to less cost intensive offshore wind measurements .

## LES Model Set-up

Large-eddy simulation is at present the most efficient technique available for high Reynolds number flow simulations, such as for atmospheric boundary layer simulations, in which the larger scales of motion are resolved explicitly

**Tab. 1:** Summary of the large-eddy simulation setup:  $L_x, L_y, L_z$  are the widths of the computational domain,  $N_x, N_y, N_z$  are the numbers of grid points and  $\Delta x, \Delta y, \Delta z$  define the grid size in the x-, y- and z-directions, respectively.

$(u_g, v_g)$	$L_x \times L_y \times L_z$ [m <sup>3</sup> ]	$N_x \times N_y \times N_z$	$\Delta_x \times \Delta_y \times \Delta_z$ [m <sup>3</sup> ]
(14, 0)	2560x1280x1371	512x256x152	5x5x5

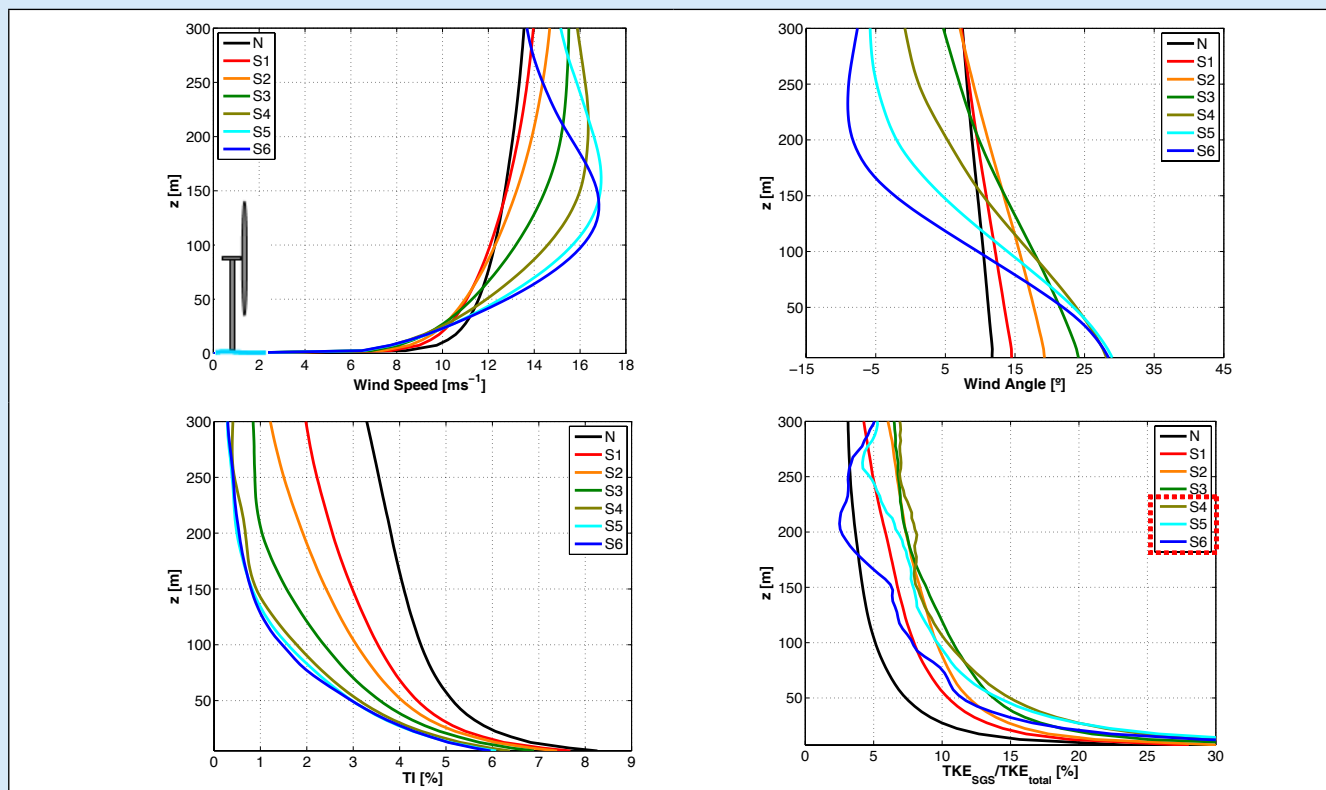


**Fig. 1:** Evolution of the mean profiles as surface cooling increases: wind speed (left-side upper panel), wind angle (right-side upper panel), Turbulent Intensity (TI) (left-side lower panel) ratio between the SGS scale and the total Turbulent Kinetic Energy (TKE) (right-side lower panel) for  $u_g = 14 \text{ ms}^{-1}$ . Acronyms shown in the legend correspond to N for neutral regime and from S1 to S6 for  $\langle w'\theta' \rangle = -0.005, -0.01, -0.02, -0.03, -0.04$  and  $-0.05 \text{ mKs}^{-1}$  respectively. Note that only the first 300 m above the surface are plotted.

while the smaller ones (subgrid scale, SGS) are parameterized. Here a Parallel Large-Eddy Simulation Model (PALM) has been used. It solves the non-hydrostatic Boussinesq approximated Navier-Stokes equations and uses a 1.5-order subgrid closure scheme. Monin-Obukhov similarity theory is assumed between the surface and the first computational grid point of the model domain. For details and features of the LES code, please refer to [2] and to the online PALM documentation ([www.muk.uni-hannover.de/raasch/PALM group/PALM group.html](http://www.muk.uni-hannover.de/raasch/PALM%20group/PALM%20group.html)).

In this work, idealized marine atmospheric boundary layer simulations are performed over a flat and uniform surface where the Charnock parameterization [3] is used on the bottom-surface to characterize the sea roughness ( $z_0$ ). Initially, a neutral boundary layer is simulated, after which a progressive decreasing of heat flux at the surface (from  $-0.0$  to  $-0.05 \text{ mKs}^{-1}$ ) is applied to stratify the layer. This forcing method for developing the stable boundary layer has been previously used by several authors (e. g. [6],[7],[8]). To deal with the limited domain size of the model, cyclic boundary conditions are applied in both horizontal directions. The Coriolis parameter is set to  $f_c = 1.181 \cdot 10^{-4} \text{ s}^{-1}$ , corresponding to a latitude of about  $54^\circ\text{N}$  (where the FINO1 platform is located). The grid spacing is isotropic

along all directions except vertical, where in order to limit the number of grid points and so save computational time a stretching factor (8%) is applied above 600 m up to the top of the model where the maximum resolution allowed is 10m.

A summary of the large-eddy simulation setup (chosen according to several sensibility tests carried out) is presented in Table 1, where  $L_x, L_y, L_z$  are the widths of the computational domain,  $N_x, N_y, N_z$  are the number of grid points and  $\Delta x, \Delta y, \Delta z$  define the grid size in the x-, y- and z-directions, respectively.

### Mean and Turbulent Vertical Structure

Fig. 1 shows the vertical profiles of horizontal wind speed, wind angle, turbulent intensity and the ratio between the SGS scale and the total (resolved+subgrid) turbulent kinetic energy for  $u_g=14\text{ms}^{-1}$  geostrophic wind prescribed and as the surface heat flux decreases (starting from the neutral regime). Profiles presented are both time-averaged and averaged over horizontal directions.

From the evolution of the mean wind speed profile, there can be seen a clear increase of the shear (increase of wind speed with altitude) as the stability increases, which dis-

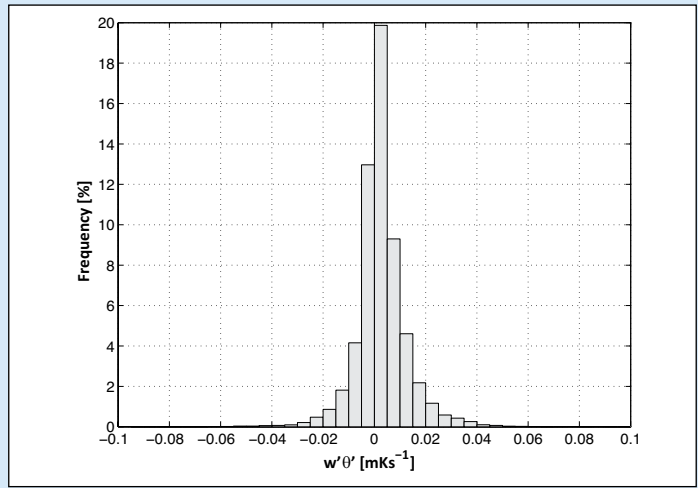


Fig. 2: Probability distribution function of sensible heat flux  $\langle w'\theta' \rangle$  for the studied period at FINO1.

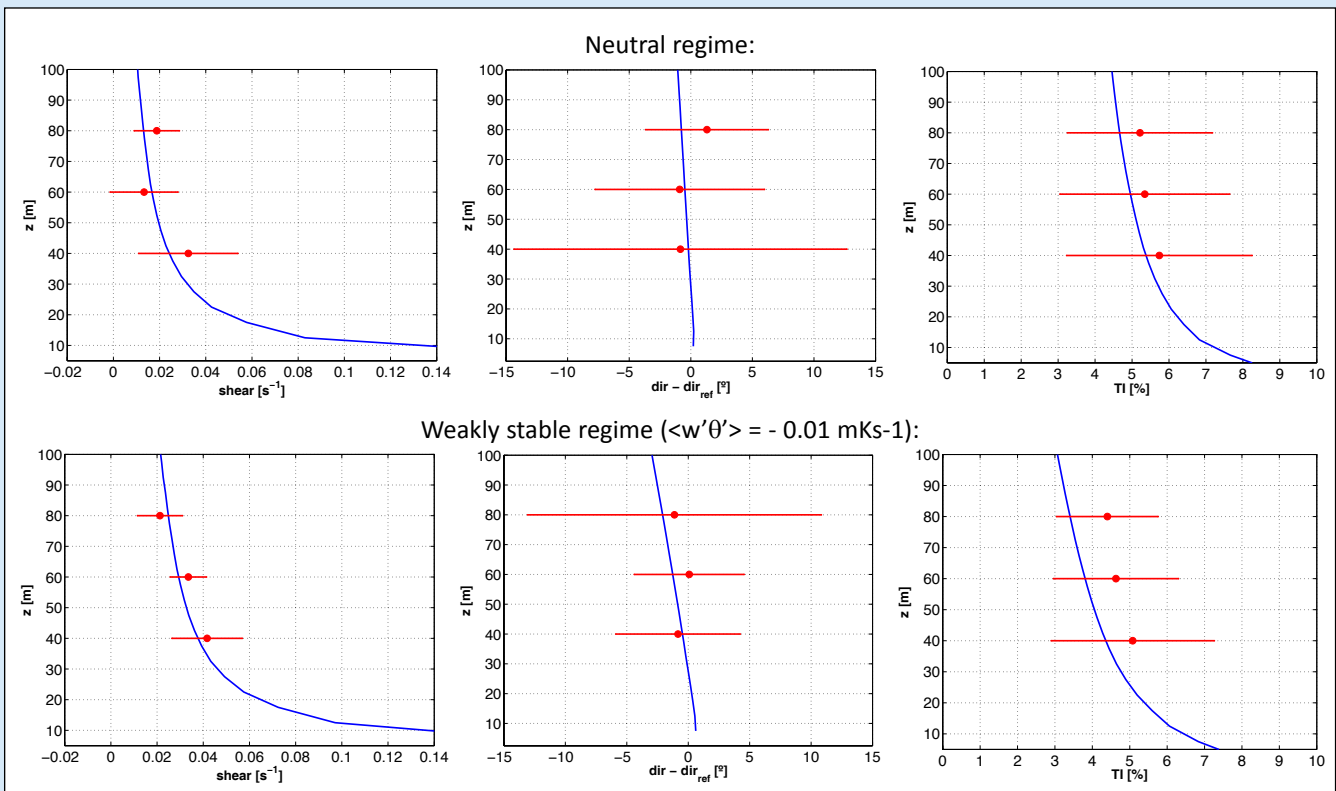


Fig. 3: Comparison of profiles between simulated (blue) and measured (red) data. Vertical wind shear (left side of the panel), horizontal wind direction (middle side of the panel) and Turbulent Intensity (TI) (right side of the panel).  $u_g = 14 \text{ ms}^{-1}$

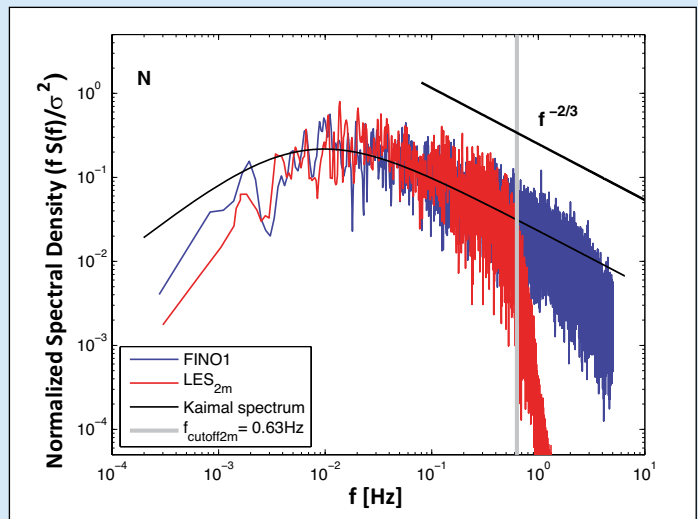
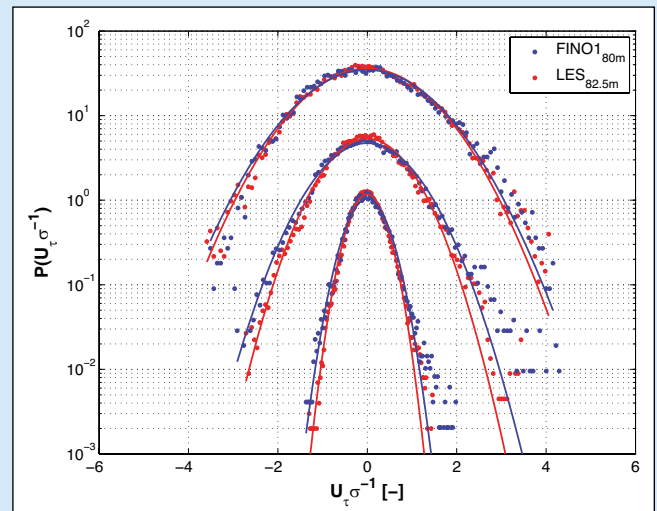


Fig. 4: Normalized one-dimensional spectra of the horizontal wind velocity fluctuations: LES simulations (red) and FINO1 data (blue). Black curve represents the Kaimal model spectrum.

Fig. 5: PDFs of velocity fluctuation increments at  $\tau = 1, 3, 10$  sec respectively (bottom-up). Red (blue) filled circles denote measured (simulated) data. The standard Gaussian distribution is indicated by solid lines. PDFs are shifted vertically by an offset of 10.



plays a low level jet (LLJ) near the top of the boundary layer in the last stage of stable profiles. Boundary layer heights range from 1140m (neutral) to about 135m (most stable cases). The angle between the surface wind direction and the geostrophic wind simulated increases with stability. Values obtained range from about  $11^\circ$  in the neutral regime to about  $30^\circ$  in the stable regime.

As expected, the turbulence intensity is strongest near the ground, decreasing from a high to zero. An evident reduction of the turbulent intensity occurs stability increases is apparent.

It is well known that the size of the dominant turbulent eddies decreases as the atmospheric stability increases and therefore small grid resolutions are necessary in order to resolve most of the turbulent motion of the flow. Otherwise the contribution of the SGS model comes into play and the results can be quite sensitive to the type of parameterization used to represent the subgrid (SGS) scales (smaller than the grid size). Near the surface, it is expected that as the stability increases from neutral to stable, the ratio between the SGS scale and the total turbulent kinetic energy (Fig. 1, right side of the bottom-panel) should increase. It can be clearly seen that for the most stable cases simulated, the opposite is found (see profiles S4, S5, S6). This unphysical behaviour of the profiles has been found by other authors (e.g. [5], [6]) and has been attributed to a failure of the SGS model. That problem is a well-known limitation in modeling where such flow conditions are very difficult to simulate due to the intermittent nature of the turbulence. Therefore, in order to simulate the most stable cases a higher resolution should be used, however at FINO1 location such stable conditions were not found for the period used in this work (see Fig. 2).

### LES versus FINO1. Profile Comparison

In this section, the LES simulations performed in section 2 are tested along vertical profiles (bulk properties of the flow) by selecting three parameters of considerable practical interest from a wind energy perspective (wind shear, wind direction and turbulent intensity). A two year (2005-2006) database from the offshore mast FINO1 station [3]

located 45 km off Borkum Island (lat.  $54^\circ 0.870N$ , long.  $6^\circ 35.240E$ ) in the North Sea is used. The comparison is limited to the three sonic anemometers available at the FINO1 location and placed at heights of 40, 60 and 80 m. We are aware that since LES simulations carried out in this work are idealized cases, a quantitative agreement between the simulation results and the observations is not expected but this will give us a guide to the relative performance and sensitivity of the model.

### Data Selection for Comparison Purposes

In order to perform the comparison between observations (FINO1) and the idealized LES simulations, FINO1 database is classified as follows:

- First, FINO1 surface heat flux data ( $\langle w'\theta' \rangle$ ) are categorized into different ranges according to the surface heat flux forcing applied in LES simulations.
- Second, the observed wind at 30 m is used (since no estimates of geostrophic winds are available from FINO1 data) to perform a sub-classification for each range of observed surface heat flux according to the simulated wind at 27.5 m (the closest height to 30m). Moreover, rain-period and humidity above 70% are excluded.

Fig. 3 shows the profile comparison for neutral and weakly stable regimes. FINO1 data are depicted as bin-median values with bars representing one standard deviation of the data in each data range.

Atmospheric measurements reveal a rather large scatter. This can be explained mainly by the complex interplay of different forces in the real atmosphere. Nevertheless, the qualitative agreement between both sets of data is rather good with most of the simulation results falling within the error bars of the FINO1 data. Moreover, the calculation of the surface heat fluxes from the FINO1 data used for the data classification is in some way not free of uncertainties and this can generate some discrepancies in the classification as well as the way of data classification itself.

On the other hand, LES simulations have also several uncertainties and their results are sensitive to grid resolution and initial conditions, amongst others, especially under stable

conditions. Therefore, LES simulations must be considered also with bars.

### Further Analysis: Time Series

The profile comparison performed in section 3 provided a measure of the mean characteristics of turbulent flow, although when information about unsteadiness (eddy structures) is desired, a statistical approach is required and therefore a time series is needed.

For this purpose, one point at the centre of the LES domain has been selected to generate time series at 80 m of the horizontal wind velocity components (longitudinal ( $u$ ), transverse ( $v$ )) to compare with one-point FINO1 measurements. A neutral simulation with  $u_g = 10 \text{ ms}^{-1}$  and 2 m grid resolution was performed. Model set-up was as described in section 2.

### Comparison between 2 m resolution LES simulation and FINO1 data

The power spectrum density obtained from the FINO1 data and LES simulation (2m resolution) is shown in Fig. 4 under neutral regime. The black line shows the theoretical slope of the Kolmogorov inertial sub-range ( $f^{-2/3}$ ). The vertical gray line is a roughly estimated cut-off frequency ( $f_{\text{cutoff}}$ ) for the LES simulation which corresponds to the frequency at which the results of LES begin to decline in comparison with measurements. Theoretically, the simulation cannot predict frequencies higher than  $f_{\text{cutoff}}$ .

As it can be seen in Fig. 4, due to the limited resolution of the grid, the turbulent spectra from the LES simulation do not show the extended inertial range found in the measured data. However, at low frequencies, the spectral shape of the simulation follows measurements reasonably well.

Moreover, the statistics of velocity increments ( $U_\tau(t) := U(t + \tau) - U(t)$  where  $U_\tau(t)$  denotes the wind speed at time  $t$  and scale  $\tau$ ) are investigated in order to characterize the flow gust behavior [10]. In Fig. 5 the probability density functions (PDFs) of the normalized  $U_\tau$  for different  $\tau$  values are shown. It should be mentioned that both data were filtered by using a top-hat filter at the cut-off frequency ( $f_{\text{cutoff}}$ ).

It is evident from Fig. 5 that, LES simulation is able to reproduce fairly the 'intermittent' of the flow. However, FINO1 PDFs show more open tails than LES values suggesting higher extreme values present in FINO1 data. This discrepancy may be partly attributed to the grid resolution.

### Conclusion

In this work LES model performance has been presented and tested with observational data through vertical profiles as well as statistical approach in order to get a more complete picture of the flow.

Notwithstanding the difficulty in interpreting the different nature of both datasets ('idealized' simulation with observational data), they generally show good qualitative agreement with some differences that can be mostly explained by the sensitivity of the data to initial conditions, subgrid parameterization (SGS model), data classification procedure and measurement uncertainties. In terms of gaining a

physical understanding of the marine atmospheric boundary layer, it is encouraging that the LES produces the same overall behavior as seen in the experimental observations.

### Acknowledgements

This has been supported by ModObs, Marie-Curie Early Stage researcher program (MRTN-CT-2005-019369), financed by European Commission.

---

### References:

- [1] DEWI GmbH Deutsches Windenergie-Institut. Wind energy study 2008. assessment of the wind energy market until 2017. Technical report, DEWI, 2008.
- [2] S. Raasch and M. Schröter. Palm: A large-eddy simulation model performing on massively parallel computers. *Meteorologische Zeitschrift*, 10:363–372, 2001.
- [3] T. Neumann, K. Nolopp, and K. Herklotz. First operating experience with the fino1 research platform in the North Sea. *DEWI Magazin*, 24, 2004.
- [4] H. Charnock. Wind stress over a water surface. *Quarterly Journal of the Royal Meteorological Society*, 81:639–640, 1955.
- [5] P. J. Mason and S. H. Derbyshire. Large-eddy simulation of the stably-stratified atmospheric boundary layer. *Boundary-Layer Meteorology*, 53:117–162, 1990.
- [6] E. M. Saiki, Chin-Hoh, and Peter P. Sullivan. Large-eddy simulation of the stably stratified planetary boundary layer. *Boundary-Layer Meteorology*, 95:1–30, 2000.
- [7] F. Ding, S. P. Arya, and Yuh lang Lin. Large-eddy simulations of the atmospheric boundary layer using a new subgrid-scale model ii. weakly and moderately stable cases. *Environmental Fluid Mechanics*, 1:49–69, 2001.
- [8] M. A. Jiménez and J. Cuxart. Large-eddy simulations of the stable boundary layer using the standard kolmogorov theory: Range of applicability. *Boundary-Layer Meteorology*, 115:241–261, 2005.
- [9] IEC61400-1. Wind turbines-part 1: Design requirements. Technical report, International Electrotechnical Commission (IEC), 2005.
- [10] J. Peinke, S. Barth, F. Böttcher, D. Heinemann, and B. Lange. Turbulence, a challenging problem for wind energy. *Physica A*, 338:187–193, 2004.